Dam-break flow regime over mobile beds, a numerical CFD approach

Alireza Khoshkonesh, Ph.D. in hydraulics, water structures, department of water engineering, Bu-Ali Sina university, Hamedan 65178, (Islamic republic of Iran)
Email: alirezakhshknsh42@gmail.com
Fariba Ahmadi Dehrashid*, Ph.D. student in hydraulics, water structures, department of water engineering, Bu-Ali Sina university, Hamedan 65178, (Islamic republic of Iran)
Email: faribaahmadi91@gmail.com
Blaise NSOM, Université de Bretagne Occidentale. IRDL/UBO UMR CNRS 6027. Rue de Kergoat, 29285 Brest, France
Email: blaise.nsom@univ-brest.fr
Saeed Gohari, Assistant professor of hydraulics structures, Department of Water Engineering, Faculty of Agri-culture, Bu-Ali Sina University, Hamedan, 65178, (Islamic republic of Iran)
Email: s.gohari@basu.ac.ir
Hossein Banejad, Associate professor of hydraulics, department of water engineering, college of agriculture, Fer-dowsi university of Mashhad, Mashhad, 91735 (Islamic republic of Iran)
Email: banejad@um.ac.ir
Payam Heidarian, MSc in water and hydraulic structures engineering, Department of hydraulic structures, Faculty of civil and environment engineering, Tarbiat Modares University, Iran
Email: pym.heidarian@gmail.com

Abstract
In this paper, the effect of the sediment bed elevation on dam-break flow over mobile beds is scrutinized using the volume of fluid (VOF) method. While the equations of motion are tackled employing the finite-volume, standard k-ε closure model and the van Rijn bed load formula. The results show that an increase in the downstream bed elevation leads to reducing: a) the flow advancing distance and water rising over the end wall, b) the sediment transport rate downstream and c) the reservoir releasing rate. Further, the decrease in level-difference results in in-creasing the sheet-flow height. However, it does not affect the critical specific downstream of the dam. It causes the formation and evolution of two hydraulic jumps and scour holes in the near field and the downstream channel. The dimen-sions of the first scour hole are larger than the second one.

Keywords
Dam-break, Bed elevation, RANS, Mobile-bed, VOF.

Introduction

Apart from the environmental effects of the dam construction such as salinity in soil and underground water, the dam-break could be caused many life and property loss-es across the downstream region (Sallam et al. (2018)., samad et al. (2018)). Sediment eroded from the drainage catchment is trapped in the dam reservoir (Zhang et al. (2019)., Hirt and Nichols (1981)). In this connection, the effect of the bed initial elevation and material on the dam-break flow characteristics has been studied rarely (Hirt and Nichols (1981)., Nsom et al. (2019)., Khoshkonesh et al. (2019)., Lobovský et al. (2014)., Leal et al. (2002)., Capart and Young (1998)., Van Rijn (1984)).

Materials and Methods

The dam-break flow characteristics are scrutinized by following process: (i) tracking the free-surface by standard VOF method using Flow-3D package; (ii) calculation of fluid pressure by implicit method; (iii) simulating the turbulent flow through the standard k-ε model; (iv) evaluation the bed-load transport using van Rijn formula (Van Rijn (1984)).

Results

The cells diameter dc and the turbulence models considered as sensitivity analysis parameters (tables 1&2). The models performance in predicting the flow depth was evaluated using dam-break experiments (Lobovský et al. (2014)., Leal et al. (2002)). NRMSE values between 0 and 0.1, 0.1 and 0.2, 0.2 and 0.4 present perfect, proper and average fit, respectively.

Table (1). The NRMSE of the mesh cells mean diameter dc and turbulence models in the dam-break experiment [Lobovský et al. (2014)]

duration of the dam-break t (s)	model A: 12.5-10				model B: 25-20			
	0.16	0.28	0.37	0.45	0.16	0.28	0.37	0.45
NRMSE values	0.0385	0.0262	0.0995	0.0565	0.0389	0.0329	0.0471	0.0639
k-ε					0.0389	0.0329	0.0471	0.0639
k-w					0.0434	0.0322	0.0471	0.0813
RNG					0.0434	0.0329	0.0471	0.0813

Table (2). The NRMSE of the van Rijn formula in the case dc = 25-20 [Leal et al. (2002)]

	model D : sand bed		model E : pumice bed	
duration of the dam-break t (s)	1	2	1	2
Van Rijn formula NRMSE	0.036	0.043	0.064	0.048

In tables 1&2, the model performance in predicting the flow depth is perfect. Whilst the computational efforts and the accuracy in d_c = 25mm and k-ε model are lesser and higher than the other cases, respectively. The van Rijn formula [Van Rijn (1984)] shows high accuracy in predicting the bed profile (table 2). Where the initial bed elevation in the downstream H_{d0} is equal to zero, then $r_s = H_{d0}/ H_{u0} = 0$. Where it is equal to upstream H_{u0}, then $r_s = 1$.

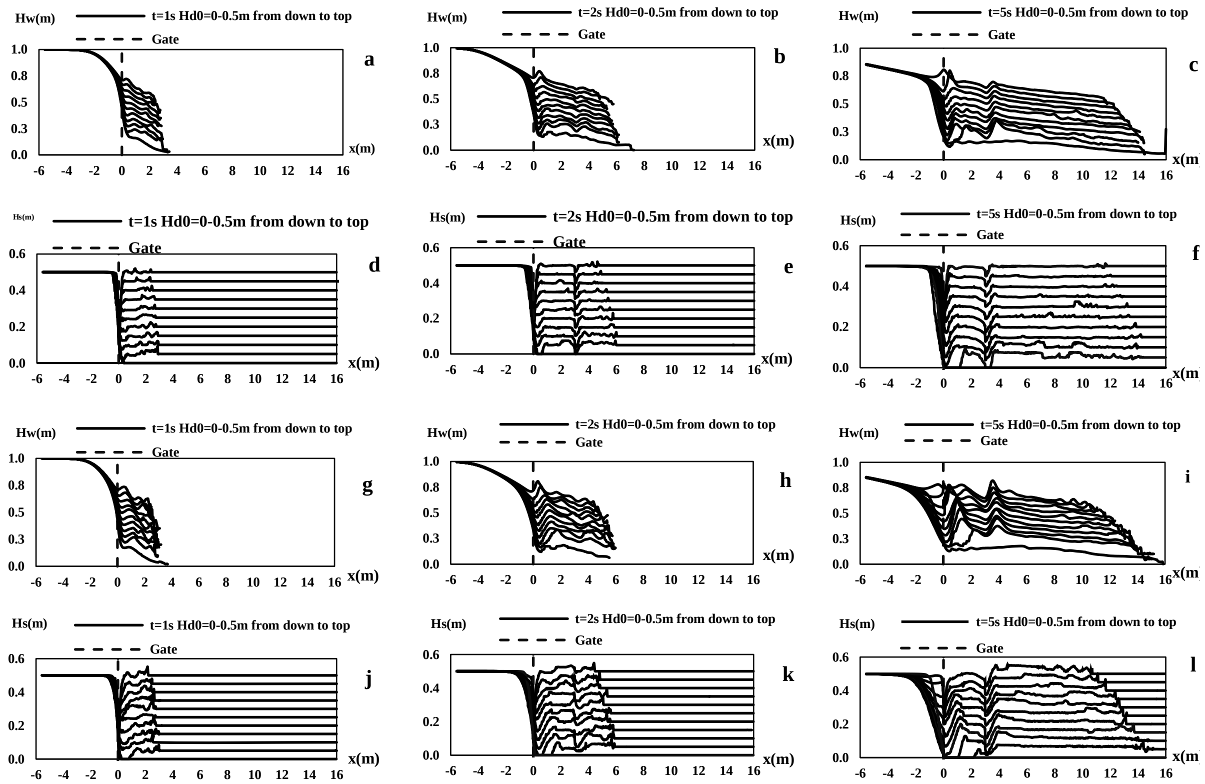

Figure (1). Evolution of free-surface and bed profiles of (a-f): sand bed; (g-l): pumice bed at *t* = 1s, 2s &5s

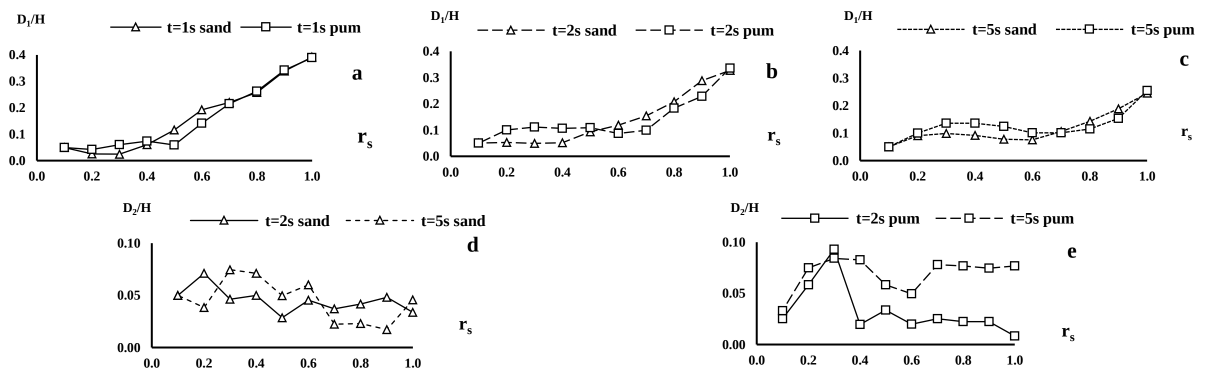

Figure (2). a-c: the first scour hole depth D_1, d: the second scour hole depth D_2 at *t*= 1s, 2s & 5s

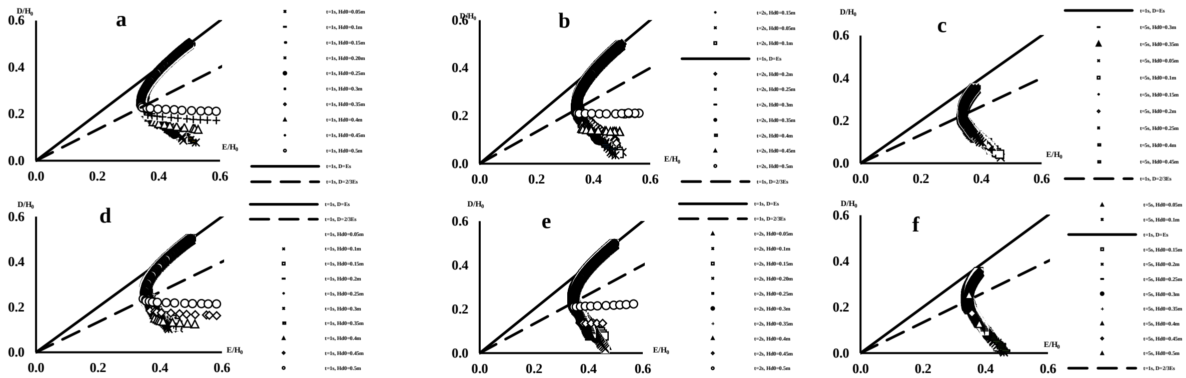

Figure (3). flow depth – specific energy of sand and pumice models in the downstream near field at t = 1s, 2s & 5s

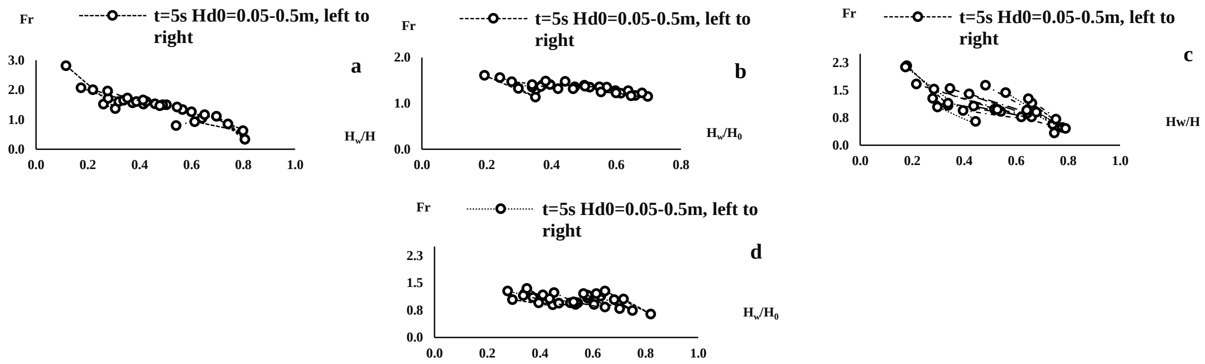

Figure (4). Froude number of the a,b: first jump and c, d: the second jump in (r_s = 0.1 – 1)

Discussion

In figs. 1a-1c & 1g-1i, reducing r_s results in rising the wave-front advancing distance x_f. However, x_f values in sand is higher than the pumice because of higher mobility of pumice than the sand. An increase in r_s leads to rising the free-surface height H_w in the downstream. Further, two hydraulic jumps are formed at the downstream. In this connection, the plausible reasons are flume length (32m), bed resistance and wall effects. Besides, rising r_s leads to increasing the height of the second jump. The greatest height of the first jump (r_s = 0.3) is about 0.36H_0. Two scour holes are formed under the two jumps, because the flow shear stress exceeds the critical value of the bed. However, the deposition occurs in 0 < x < 3m. The second hole emerges in x ≈ 3m. The result is not reported in (Sallam et al. (2018)., samad et al. (2018)., Zhang et al. (2019)., Hirt and Nichols (1981)., Nsom et al. (2019)., Khoshkonesh et al. (2019)., Lobovský et al. (2014)., Leal et al. (2002)., Capart and Young (1998)). In fig. 2a, D_1 is increased by increment r_s at t = 1s. In figs 2b & 2c, sand and pumice diagrams are sleep reverse S-shape. An inflection point is observed in r_s = 0.5 and r_s = 0.7. While D_1 values in pumice are greater than the sand in $r \leq 0.5$, there is a reverse trend in at $r \geq 0.6$. In figs 2d & 2e, the diagrams of D_2 are irregular, while D_{2max} is about from the order of 1/5 the D_{1max}. In figs 3a-3f, the ascending sections are roughly identical in the sand and pumice. Therefore, the subcritical flow within the reservoir does not dependent on the bed material. The least specific energy value in all diagrams is equal to $E_c \approx 0.35$m. Hence, bed elevation does not affect the E_c values. The D/H_0 values are increased through the increment of the r_s in the descending section. In fig. 4, each diagram is embodying three distinctive parts ((H_w/H_0)$_1$), crest ((H_w/H_0) $_2$), and end-points ((H_w/H_0)$_3$) of the hydraulic jump. In fig. 4a, the flow regime is changed from super- to subcritical by rising the r_s. Indeed, the diagrams are displaced to the right side of the H_w/H_0 axis. Therefore, the greatest and least Froude number values are equal to Fr_{max} = 2.8 in r = 0.1 and Fr_{min} = 0.33 in r = 1, respectively. In return, in fig. 54, the flow regime remains supercritical. In this figure the Fr_{min} is over than 3.5 times the corresponding value in fig. 4a. It means that the velocity at the crest of the second hydraulic jump is considerably higher than the first one. In fig. 4c, the flow regime is changed from super- to subcritical. In fig. 4d, the flow regime transforms from super- to subcritical.

Conclusions

The modeling results showed: rising the downstream bed elevation leads to a) increas-ing the water free-surface height in the downstream, b) reducing the wave front ad-vancing distance to the downstream and rising water over the end-wall c) reducing the reservoir releasing rate. Likewise, two hydraulic jumps are formed at the downstream of the dam in all cases except the downstream with fixed-bed. Two scour holes ap-pear under the first and second jumps. The depths of the holes are diminished by increment of the downstream bed elevation. Likewise, the range of the Froude num-ber in the first jump is higher than the second one. Rising the bed elevation leads to changing the flow regime from super- to subcritical in jump regions. Ultimately, VOF has high accuracy in predicting the characteristics of the dam-break flow over mobile beds.

References

Ahadiyan, J., Adeli, A., Bahmanpouri, F., Gualtieri, C., Khoshkonesh, A. (2021). Riprap ef-fect on hydraulic fracturing process of cohesive and non-cohesive coastal protective levees. *Water Resource Management*.

Amini A, Arya A, Eghbalzadeh A, Javan M. (2017). Peak flood estimation under overtopping and piping conditions at Vahdat Dam, Kurdistan Iran. *Arab J Geosci*. 10(6), 1–11.

Bahmanpouri, F., Daliri, M., Khoshkonesh, A., Montazeri Namin, M., Buccino, M. (2020). Bed compaction effect on dam break flow over erodible bed; experimental and numerical modeling. Journal of Hydrology, 125645.

Banejad, H., Heydari, M., Khoshkonesh, A. (2015). The comparison of the performance of single-equation models of turbulence kinetic energy and two k-e equation models in hydrau-lic simulation of dam failure on the mobile bed. *International Conference on Modern Re-search in Agricultural Science and Environment, December 15th, Malaysia, Kuala Lumpur*

Capart H, Young DL. (1998). Formation of a jump by the dam-break wave over a granular bed. *J Fluid Mech*. 372, 165–87.

Hirt CW, Nichols BD. (1981). Volume of fluid (VOF) method for the dynamics of free boundaries. *J Comput Phys*. 39(1), 201–205.

Fraccarollo L, Toro EF. (2012). Experimental and numerical assessment of the shallow water model for two-dimensional dam-break type problems. Evaluation expérimentale et numérique. *J Hydraul Res*. 37–41.

Heydari M, KhoshKonesh A. (2016). The comparison of the performance of Prandtle Mixing Length, Turbulence Kinetic Energy, K-e, RNG and LES turbulence models in simulation of the positive wave motion caused by dam break on the erodible bed. *Indian J Sci Technol*. 9(7).

Khoshkonesh, A., Nsom, B., Bahmanpouri, F., Ahmadi Dehrashid, F., Adeli, A. (2021). Numerical study the dynamic and structure of partial dam-break flow using VOF method. Water Resource Management.

Khoshkonesh, A., Nsom, B., Gohari, S. and Banejad, H. (2019). A comprehensive study on dam break flow over dry and wet beds. *Ocean Engineering*, 188:106279.

Khoshkonesh, A., Gohari, S. and Banejad, H. (2019). Numerical Study of the effect of the flood-plain obstacles on dam-break flow by MPS method. *Journal of Water and Soil Conservation*. 26(6): 119-138. http://doi.org/ 10.22069/JWSC.2019.16153.3141.

Khoshkonesh, A., Nsom, B., Ahmadi Dehrashid, F., Heidarian, P., Riaz, Kh. (2021). Com-parison of the SWE and 3D models in simulation of the dam-break flow over the mobile bed. *5th the scientific conference of applied research in science and technology of Iran. Sep-tember 5th 2021.*

Khoshkonesh, A., Gohari, S. and Banejad, H., Ahmadi Dehrashid, F., Bajelvand, S. (2020). Kinematic analysis of dam-break flow over granular beds. *National Conference on Water Technology Development, Watershed Management and River Engineering, March 5th , Tehran University, Tehran.*

Lobovský, L., Botia-Vera, E., Castellana, F., Mas-Soler. (2014). Experimental investigation of dynamic pressure loads during dam break. *J. Fluids Struct.* 48, 407–434.

Leal JGAB, Ferreira RML, Cardoso AH. Dam-break wave propagation over a cohesionless erodible bed. XXX IAHR Congr. 2003;(2002).

Nsom, B., Latrache, N., Ramifidisoa, L., Khoshkonesh, A. (2019). Analytical Solution to the Stability of Gravity-driven Stratified Flow of Two Liquids over an Inclined Plane, in: *24th French Mechanics Congress in Brest. Brest*, p. 244178.

Rijn, L.C. van. (1984). Sediment transport, part I: bed load transport. *J. Hydraul. Eng.* 110, 1431–1456.

Sallam A, Bader Alharbi A, Usman ARA, Hussain Q, Ok YS, Alshayaa M, et al. (2018). Environmental consequences of dam construction: a case study from Saudi Arabia. *Arab J Geosci*.11(3).

Samad N, Chauhdry MH, Ashraf M, Saleem M, Hamid Q, Babar U, et al (2016). Sediment yield assessment and identification of check dam sites for Rawal Dam catchment. *Arab J Geosci* [Internet].9(6). Available from: http://dx.doi.org/10.1007/s12517-016-2484-9

Zhang W, Chen Y, Yang B quan, Zhang L, Zhang C, Liu X qiang. (2019). Experimental and numerical analyses on working performance of a high arch dam with deep-seated joints: Yebatan arch dam, China. *Arab J Geosci*. 12(4).